Modeling of ion-cyclotron resonant heating in Wendelstein 7-X equilibrium

2014 J. Phys.: Conf. Ser. 561 012006

(http://iopscience.iop.org/1742-6596/561/1/012006)

Journal of Physics: Conference Series **561** (2014) 012006 doi:10.1088/1742-6596/561/1/012006

Modeling of ion-cyclotron resonant heating in Wendelstein 7-X equilibrium

J.M. Faustin, W.A. Cooper, J.P. Graves, D. Pfefferlé
Ecole Polytechnique Fédérale de Lausanne (EPFL), Centre de Recherches en Physique des Plasmas (CRPP), CH-1015 Lausanne, Switzerland

Abstract. W7X stellarator 3D equilibrium has been computed with the equilibrium code ANIMEC (Anisotropic Neumann Inverse Moments Equilibrium Code). This equilibrium was used to model ICRH minority heating in ^{4}He(H) plasma with the 3D full-wave code LEMan (Low frequency ElectroMagnetic wave propagation). The coupled power spatial distribution is shown for different resonance positions within the range of frequencies foreseen for the ICRH antenna. It is found that for the high mirror equilibrium examined, the antenna frequency can be chosen to optimise the power deposition in the plasma core while limiting the absorption at the edge.

1. Introduction

Wendelstein 7-X (W7X) is a large superconducting quasi-isodynamic stellarator under construction in Greifswald, Germany. This fully optimised device aims at demonstrating the feasibility of operating steady state plasmas relevant for a fusion powerplant while assuring the confinement of fast particles. Several sources of heating will be mixed in W7X in order to reach fusion plasma relevant temperatures. An assessment of the viability of ion-cyclotron resonance heating (ICRH) applied to W7X constitutes an important step to determine whether this approach is feasible. The design of antennas for this method of heating relies heavily on ICRH simulations in quasi-isodynamic stellarator systems.

Numerical simulations using three-dimensional codes were performed to compute a W7X relevant equilibrium and wave propagation in the ICRH range of frequency. A high-mirror equilibrium was produced using the equilibrium code ANIMEC (Anisotropic Neumann Inverse Method Equilibrium Code) [1]. The full-wave code LEMan (Low frequency ElectroMagnetic wave propagation) [2] uses this equilibrium to solve the wave equation to 0th order in Larmor radius including warm contributions to the dielectric tensor. LEMan is therefore limited to the calculation of fundamental minority heating scenarios. According to Ref. [3] in particular one of the antenna designs foreseen for W7X cover a range of frequencies valid for fundamental minority heating of H in D or ^{4}He, which are scenarios LEMan can compute. However the neutrons generated by D-D fusion reactions may activate the machine which renders deuterium a less desirable majority species for ICRH scenarios for machine maintenance purposes. Consequently we will focus here on ^{4}He(H) plasmas.

This paper is organised as follow. Section 2 describes the main features of the equilibrium case on which the wave propagation is based. In section 3 we discuss the plasma parameters and the scan perfomed in the wave calculation. In section 4 we present the power deposition on the fast ion fraction of the minority species.

2. 3D Equilibrium

The ANIMEC code is used to compute an anisotropic W7X fixed boundary 3D geometry plasma equilibrium. Many toroidal mirror configurations are accessible with a proper use of the modular and planar coils. In this study, we relied on the so-called high mirror configuration which offers the potential for α-particle confinement in a reactor-scaled device. This configuration is of particular interest insofar as ICRH will be used in W7X not only to investigate plasma heating but also to generate a fast particle population to emulate the behaviour of α-particles in a reactor.

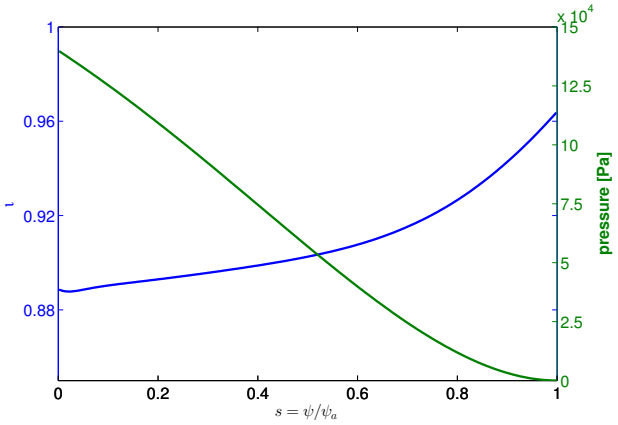

Figure 1. Rotational transform $\iota(s)$ and pressure $p(s)$ profiles used for the equilibrium calculation.

The rotational transform, and the plasma pressure used in input is shown in Figure 1, where s refers to the radial variable. Note that s is proportional to the toroidal magnetic flux ψ and proportional to the enclosed plasma volume. The equilibrium magnetic field amplitude for different toroidal angles, displayed in Figure 2, is obtained and gives a toroidal mirror ratio defined as [4] :

$$\frac{B_{\varphi=0} - B_{\varphi=\pi/5}}{B_{\varphi=0} + B_{\varphi=\pi/5}} = 8.5\% \tag{1}$$

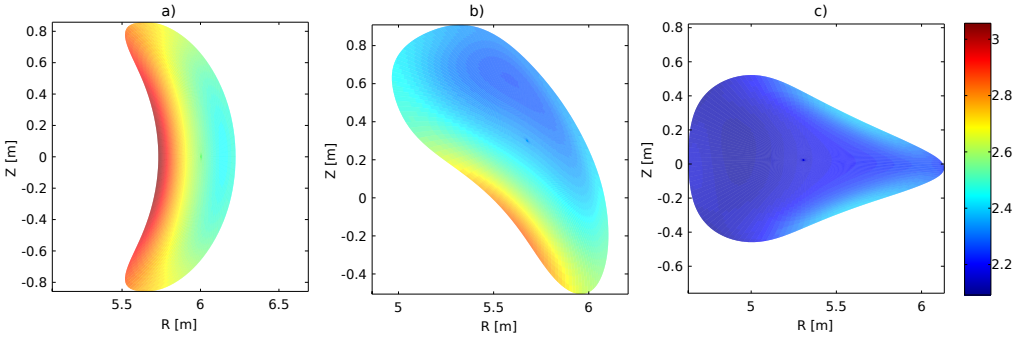

Figure 2. Magnetic field amplitude [T] for three cross section between the two symmetry planes : a) $\varphi = 0$, b) $\varphi = \pi/10$, c) $\varphi = \pi/5$.

An important feature of this high mirror equilibrium for the wave propagation is that the minimum magnetic field in the bean-shaped cross section is higher that the maximum magnetic field in the triangular cross section (respectively a) and c) in Figure 2), i.e. there is no available wave frequency which corresponds to a resonant magnetic field at every toroidal angle. This will be clearly illustrated in the next section. Finally, The ANIMEC code uses a bi-Maxwellian model [1] to incorporate the contribution of hot particles to the equilibrium. The anisotropy was chosen to be constant and set to $T_\perp/T_\parallel = 3$, thus envisaging strong perpendicular ICRH heating.

Now that the plasma equilibrium has been presented we will focus on the wave field calculation.

3. 3D Wave field

On the basis of the ANIMEC equilibrium converted to Boozer coordinates, the 3D full-wave code LEMan computes the wave field. LEMan solves the Maxwell's equations in terms of scalar and vector potentials ϕ and $\mathbf{A}$ respectively, which take the following form in fourier space :

$$\nabla^2\mathbf{A} + \left(\tfrac{\omega}{c}\right)^2 \hat{\epsilon}\cdot\mathbf{A} + i\tfrac{\omega}{c}\hat{\epsilon}\cdot\phi = -\tfrac{4\pi}{c}\mathbf{j}_{ant} \tag{2}$$

$$\nabla\cdot(\hat{\epsilon}\cdot\nabla\phi) - i\tfrac{\omega}{c}\nabla\cdot(\hat{\epsilon}\cdot\mathbf{A}) = -4\pi\rho_{ant} \tag{3}$$

Here c stands for the velocity of light and $\hat{\epsilon}$ is the warm dielectric tensor. The elements of this tensor are derived from a Maxwellian distribution function for the electrons and the background species and the same bi-Maxwellian model that in the ANIMEC code for the fast fraction of the minority species [6]. Note that this set of equations has been obtained by introducing the Coulomb Gauge ($\nabla\cdot\mathbf{A} = 0$). The problem is then discretised using finite elements in the radial direction and Fourier harmonics in the poloidal and toroidal directions [2]. The subscripts *ant* refers to the source contributions, namely the charge density and the current density flowing in the antenna. The geometrical description of the antenna is a crucial aspect of the wave calculation. In LEMan, the current density takes a divergence-free form :

$$\mathbf{j}_{ant} = \nabla s \times \nabla\sigma(s,\theta,\varphi) \tag{4}$$

The function $\sigma(s,\theta,\varphi) = \sigma_s(s)\sigma_\theta(\theta)\sigma_\varphi(\varphi)$ contains the geometrical aspect of the antenna and gives a degree of freedom concerning its localisation and extension around the torus. A realistic antenna would be localised between two poloidal and toroidal angles and would even introduce phase shifts between current straps but would excite a broad Fourier mode spectrum. Instead we choose an antenna localised only radially at the edge of the plasma domain, which encloses the whole torus and excites only one mode ($m_{ant} = 3, n_{ant} = 15$). This model, although less realistic offers the first satisfactory results concerning the wave absorption for ICRH minority heating scenarios computed in W7X. Using this simplified antenna also allows us to take advantage of the 5-period symmetry of the device. Therefore the wave simulations were run only in one fifth of the full torus, limiting our toroidal angle domain between 0 and $2\pi/5$. Note that the antenna current density prescribed in LEMan should in principle be multiplied by a constant in order to account for the real value of the power coming from the antenna and coupled to the plasma. Therefore LEMan uses and computes only normalised quantities such as the power absorption results shown in the next section. LEMan computes in particular the power absorbed in the plasma inside each magnetic surface labeled s, the power coupled by the antenna in the same

region and the Poynting vector, which read respectively [6] :

$$P_{pla}(s) = \frac{\omega}{8\pi}\int_{s'<s} \mathrm{d}V' \left(|\mathbf{B}|^2 - \mathbf{E}^*(\cdot\hat{\epsilon}\cdot\mathbf{E})\right) \quad (5)$$

$$P_{ant}(s) = \frac{i}{2}\int_{s'<s} \mathrm{d}V' \left(\mathbf{E}^*\cdot\mathbf{j}_{ant}\right) \quad (6)$$

$$S_{Poynt} = \frac{c}{8\pi}\int_{s} \mathrm{d}\mathbf{S}\left(\mathbf{E}^*\times\mathbf{B}\right) \quad (7)$$

where $\mathbf{B}$ and $\mathbf{E}$ are respectively the magnetic and electric wave fields. These quantities are used in LEMan in order to check the power balance $P_{pla}(s) = P_{ant}(s) + iS_{Poynt}$. A quantitative calculation of the power deposition can be performed using a particle code like VENUS-LEVIS [7].

In the following, the plasma is composed of ^{4}He with 5% of H minority. The central density is chosen as $n_{e0} = 8\times10^{19}\,m^{-3}$ and the profile takes the form $n_\alpha(s) = n_{\alpha 0}\left(0.99(1-s^4)^4 + 0.01\right)$, where α refers to the different electronic and ionic species in the plasma. This particular choice of density profile has a very low plasma density at the antenna, which is similar to the experimental setup where some gas is puffed near the antenna to tunnel the wave into the plasma The temperature profile is prescribed as $T_e = T_i = T_0(1-s)$ where $T_0 = 3\,keV$ is the central temperature. Coupling waves in the ion-cyclotron range of frequencies for efficient heating purposes requires a strong minority particle-wave absorption in the plasma centre. However, for a given wave frequency the resonance can be located only near the plasma edge and can even disappear because of the toroidal dependency of the magnetic field. Therefore a scan in the wave frequency allows us to qualitatively assess an optimal range of frequencies for which the power would be mostly deposited in the plasma core. The results of this scan are presented in the following section.

4. Power deposition

The wave calculation was done with 4 different frequencies : 32 MHz, 33.8 MHz, 36.6 MHz, 39.6 MHz. The plasma is composed of H minority in ^{4}He and we focus on fundamental minority heating only. These frequencies correspond respectively to the following resonant fields : 2.1T, 2.22T, 2.4T, 2.6T. The deposited power on the fast fraction of the minority species is displayed for each case in Figure 3 and shows some interesting consequences for the magnetic equilibrium characteristics of W7X. First, as mentioned before, the wave-particle resonance disappears in a certain range of toroidal angle for each frequency because of the high-mirror configuration we chose. Then, unlike in tokamak equilibrium where the resonance lies in a Doppler shifted vertical layer, the wave-particle interaction can display a more significant radial extent allowing a better power deposition around a certain toroidal position, e.g. $B_c = 2.1T, \varphi = \pi/5$.

On the other hand, in this particular case, the toroidal range for which the power is absorbed is rather limited. Higher frequencies, corresponding in our case to 2.4T and 2.6T, have a resonant layer geometry more localised to the curved boundary, and may besides lead to operational problems. Indeed, around the triangular shaped cross section, the resonance lies very close, if not on the wall which one must avoid for machine inner component safety.

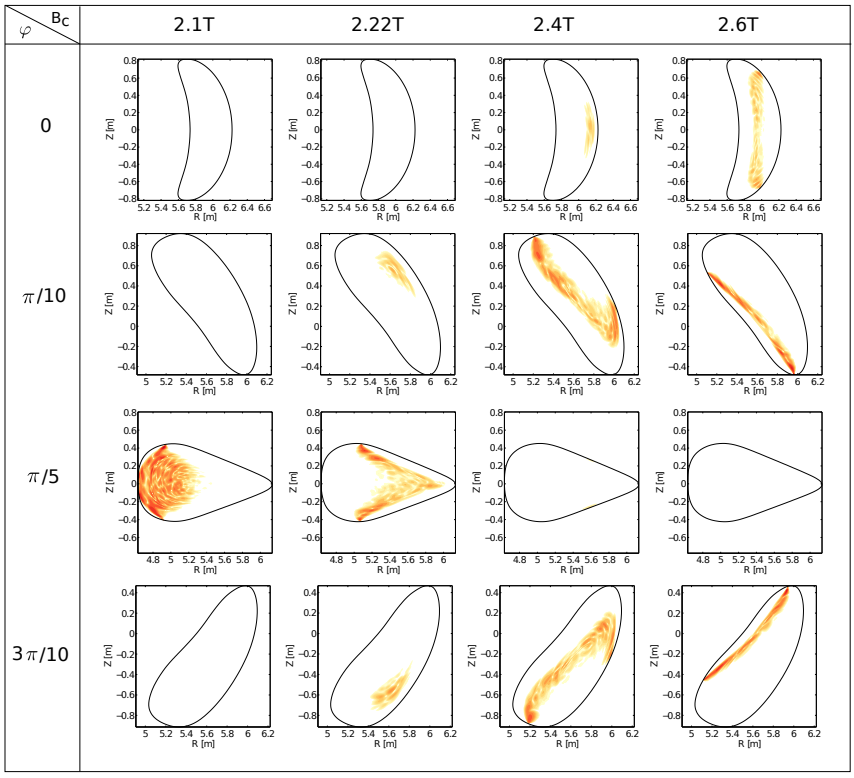

Figure 3. Power deposition in arbitrary units in the fast ion fraction of the minority species for the 4 frequencies of the scan at different toroidal angle

In Figure 4 we propose a more global diagnostic in order to describe the localisation of the power deposition around the torus. The idea is to investigate the radial and toroidal dependency of the power absorption. The radial domain is splitted into three sub-domains. Then, we integrate the absorbed power over the toroidal domain after integration over the poloidal variable and over each radial sub-domains separately. Precisely, if one calls the three-dimensional dependent deposited power density $P(s,\theta,\varphi)$, we compute the following power integrals :

$$\mathcal{P}_i(\varphi) = \frac{\displaystyle\int_{\Omega_i}\int_0^{2\pi} \sqrt{g}P(s,\theta,\varphi)\mathrm{d}s\mathrm{d}\theta}{\displaystyle\int_0^1\int_0^{2\pi}\int_0^{2\pi/5} \sqrt{g}P(s,\theta,\varphi)\mathrm{d}s\mathrm{d}\theta\mathrm{d}\varphi} \tag{8}$$

$$\text{with} \begin{cases} \Omega_1 \;\widehat{=}\; 0 \leq s \leq \dfrac{1}{4} \\ \Omega_2 \;\widehat{=}\; \dfrac{1}{4} \leq s \leq \dfrac{3}{4} \\ \Omega_3 \;\widehat{=}\; \dfrac{3}{4} \leq s \leq 1 \end{cases} \tag{9}$$

Here, Ω_i identifies a fractional volume within the plasma, i.e. Ω_1 and Ω_3 represent respectively the first and the last fourth of the plasma volume. We therefore have some information on the fraction of the power that goes to the edge of the plasma compared to that at the core.

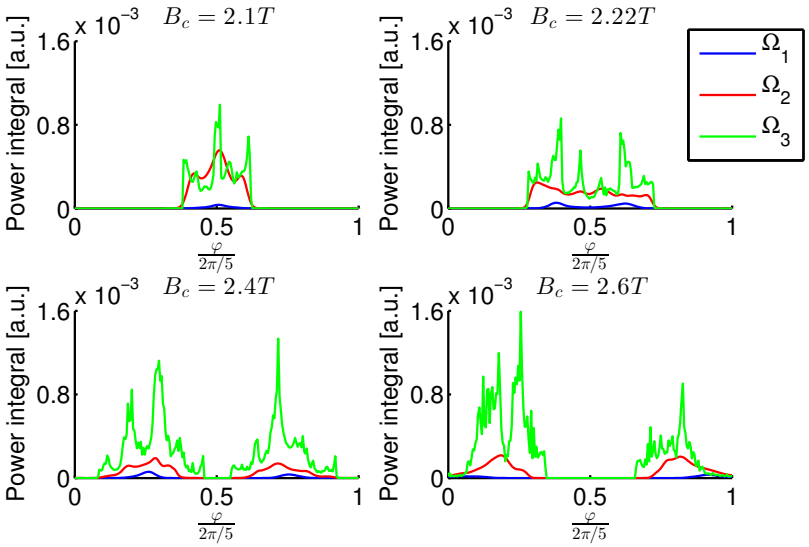

Figure 4. Power integrals computed for the three radial subdomains for the 4 frequencies of the scan as function of the normalised toroidal angle $\frac{\varphi}{2\pi/5}$.

Figure 4 shows the power integrals for each resonant field investigated and describes precisely the range of toroidal angle in which the wave transmits energy to the plasma. As the resonant field decreases this range becomes narrower. However it appears that the power deposition on the fast ion fraction of the minority species is most effective with an intermediate resonant field $B_c = 2.22T$. Indeed, it presents a toroidal range similar to the ones of higher resonant field.

In Figure 5 we plot the cumulative integration over the toroidal angle for the inner and outer radial domain, Ω_1 and Ω_3 respectively. Figure 5 shows that the $B_c = 2.22T$ case has the highest value of the power integral closest to the core flux surfaces, while limiting the relative amount of power going to the edge of the plasma. Finally it is clear that for higher resonant field, e.g. $B_c = 2.6T$, the wave-particle interaction disappears in almost half of the toroidal range and takes place mainly in the edge of the plasma with virtually no interaction in the core.

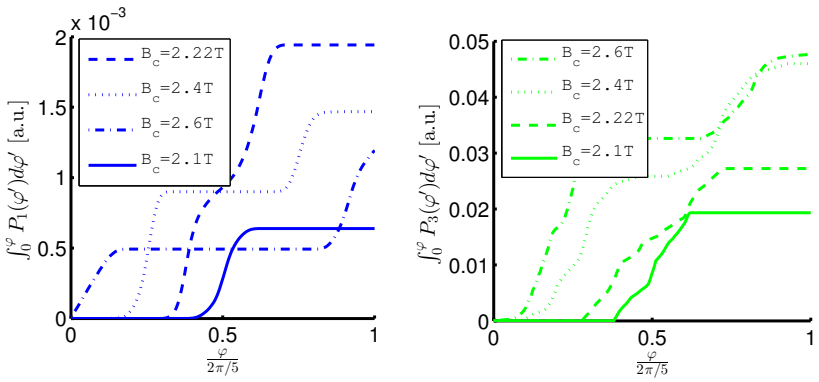

Figure 5. Cumulative integration over φ of the power integrals computed in the first and the last fourth of the plasma volume.

5. Conclusion

A 3D anisotropic high-mirror configuration W7X equilibrium was generated with ANIMEC. This equilibrium constitutes the basis for the application of by the 3D full-wave code LEMan in order to study the wave propagation in the ion-cyclotron range of frequency and the power deposition on fast minority ion fraction. A simplified antenna model was used with a single mode ($m_{ant} = 3, n_{ant} = 15$). This constitutes the first results concerning the wave absorption in an advanced stellarator system where it appears that some frequencies deposit power more efficiently on fast ions at the 0th order in Larmor radius. These preliminary calcutations indicate that a frequency of 33.8 MHz resonating with the minority species at $B_c = 2.22T$ appears to be close to optimal. Further simulations are planned with these 3D tools. For instance a more standard equilibrium, i.e. with a lower mirror ratio, will be investigated and compared to the study presented in this paper. Moreover it will be of interest to fully localise the antenna in one period therefore providing an excitation with many poloidal and toroidal modes describing a realistic antenna excitation spectrum and to study the wave propagation and absorption from that period to its neighbours.

References

[1] Cooper W A et. al. 2009 *Comput. Phys. Commun.* **180** 1524
[2] Popovich P et al. 2006 *Comput. Phys. Commun.* **175** 250
[3] Ongena J et al. 2014 *Phys. Plasmas* **21** 061514
[4] Geiger J et al. 2008 *35th EPS Conference on Plasma Phys. Hersonissos, 9-13 June 2008* **32D** 2.062
[5] Mellet N et al. 2010 *Comput. Phys. Commun.* **182** 570
[6] Mellet N 2009 *PhD Thesis n° 4398, EPFL Lausanne*
[7] Pfefferle D et al. 2014 *Comput. Phys. Commum.* **in press**